Reac Kinet Mech Cat (2018) 124:873–889
https://doi.org/10.1007/s11144-018-1375-3

Effect of copper and cerium on the performance of Ni-SBA-16 in the partial oxidation of methane

Zahra Shokoohi Shooli[1] · **Ali Izadbakhsh**[1] · **Ali Mohammad Sanati**[2]

Received: 18 December 2017 / Accepted: 16 February 2018 / Published online: 26 February 2018

Abstract In this research, the effect of Ce, Cu and Ce–Cu promoters on the performance of Ni/SBA-16 catalyst in partial oxidation of methane reaction was investigated. The Ni/SBA-16 catalyst with 9.1 wt% Ni content without promoter and Ni/SBA-16 catalyst promoted with cerium, copper, copper–cerium with equimolar to nickel content were prepared and their performance in methane partial oxidation reaction were evaluated. The prepared catalysts were characterized by XRD, N_2 adsorption and EDX-FESEM analysis techniques. The N_2 adsorption isotherms of catalyst samples showed that adding promoters to the Ni/SBA-16 catalyst partly decreased the surface area of catalysts. Furthermore, the results using XRD analysis partly demonstrated dispersion of nickel particle for catalyst Cu-promoted. Also, SEM analysis showed a similar size of nano crystallites in the range of 8–20 nm for all catalyst samples. The results of evaluation of catalytic activities of the catalysts showed high activity of unpromoted and Ce-promoted nickel catalyst in methane conversion ($\approx$ 93%) remained stable for 3 h. The effects of other reaction parameters such as temperature, gas hourly space velocity and molar ratio of the feed were also evaluated and reported.

Keywords Mesoporous SBA-16 · Nickel catalyst · Partial oxidation of methane · Syngas · Hydrogen

Electronic supplementary material The online version of this article (https://doi.org/10.1007/s11144-018-1375-3) contains supplementary material, which is available to authorized users.

✉ Ali Izadbakhsh
izadbakhsh@pgu.ac.ir

[1] Department of Chemical Engineering, Faculty of Petroleum, Gas and Petrochemical Engineering, Persian Gulf University, Bushehr, Iran

[2] Department of Environment, Persian Gulf Research Institute, Persian Gulf University, Bushehr, Iran

Introduction

Over the past few decades, the natural gas is regarded as one of the most important and attractive raw materials for the chemical industry because of the increasing concerns of the reduction of crude oil reserves, environmental considerations, huge resources of natural gas and also problems like the difficulties of its transfer to consumption centers [1].

Among the different methods of conversions of natural gas, there is a growing tendency to apply catalytic partial oxidation (CPO) of methane method. Its advantages such as exothermicity and the production of syngas of H_2/CO ratio is suitable for methanol and Fischer–Tropsch synthesis [2].

Noble metal-based catalysts [3–6] and transition metal-based catalysts [3, 7–10] were employed as catalytic materials in the partial oxidation of methane. Although precious metals such as Pd, Pt, Ru and Rh have been reported to be active and stable for transformation of methane [11, 12], high cost of these precious metals is the main drawback of their application in the conversion. Fe, Co, and Ni based catalysts as active yet cheaper alternatives catalyst for CPO of methane are investigated [13–15]. In particular, Ni catalysts have been widely investigated because of their lower cost and relatively higher activity in the POM. However, Ni-based catalysts suffer from catalyst deactivation by sintering of Ni particles [16, 17] and phase transformation of the supported solids [18] in the POM. The low cost and competitive performance of Ni-based catalysts, therefore, leads to optimization researches of these catalysts in this process.

There are various methods for increasing resistance of the nickel particles toward the coke, and as well as improving catalytic activity of those particles, which consist of addition of the promoter metals [16, 19–23] and changing the nature of the support [24–26]. The highly dispersed metallic species in the catalyst support resist stronger against to the sintering and the formation of large aggregates of the active species and the deactivation [27]. Porous supports with high specific surface area can make many active sites to improve dispersion of nickel particles. The mesoporous silica such as MCM-41 [26, 28], SBA-15 [19–22] and SBA-16 [26, 29, 30] with high surface area and almost neutral property are suitable as the supporting medium of nickel particles.

MCM-41 is one of the M41S family members developed by Mobil Oil Corporation scientists in 1992, exhibits a hexagonal arrangement of uniform mesopores whose dimensions may be engineered in the range of 15 Å to greater than 100 Å with relatively thin pore walls [31] with the striking properties such as high specific surface area, regular nano-sized pore structure.

SBA-15, a highly ordered two-dimensional (p6mm), mesoporous silica structures, which mainly comprise hexagonally arranged, parallel or twisted channels with unusually large d(100) spacing of 104–320 Å have been synthesized in the presence of triblock poly(ethylene oxide)-poly(propylene oxide)-poly(ethylene oxide) (PEO–PPO–PEO) copolymers.

SBA-15 mesoporous structures have been prepared with BET surface areas of 690–1040 m^2/g, pore sizes of 46–300 Å, silica wall thicknesses of 31–64 Å, and pore volumes as large as 2.5 cm^3/g.

SBA-16, a three-dimensional cubic ($Im\bar{3}m$) cage-structured mesoporous silica structure, with a large cell parameter (a = 176 Å), thick pore walls, a BET surface area of 740 m^2/g and a pore size of 54 Å, has been synthesized using triblock copolymers with large PEO segment [32].

The Ni/SBA-16 catalyst has shown a better regeneration performance in deep desulfurization of warm syngas in comparison to Ni/SBA-15 catalyst. The difference in performance of two those catalysts is associated with the migration of the nickel particles from structure SBA-15 support and its sintering due to the straight channel pore structure [26].

Because of the small size of SBA-16 pore diameter compared to SBA-15, nickel particle size supported on SBA-16 is smaller than those of Ni/SBA-15 catalysts, which led to the success of the catalyst Ni/SBA-16 in hydrodechlorination of 1,1,2-trichloroethane [30].

MCM-41 supported nickel particles has a high dispersion, but at high temperatures aggregation of nickel particles occurs on its surface [28]. The use of three-dimensional silica SBA-16 with the cage-like mesoporous is a suitable candidate due to the high access to gas molecules, the confinement of nickel nanoparticles in its pores and high wall thickness [26, 32].

The addition of promoter metals to supported nickel catalysts changes the interactions between the nickel with its support, which causes increasing the stability and activity of the catalyst in the reaction of methane partial oxidation. The addition of Cu promoter to the Ni/SBA-15 catalyst in the methane partial oxidation reaction has demonstrated the decreased carbon deposition due to solid solution formation. Also, the catalyst with the amount of Cu promoter less than 2.5 wt% had a higher performance and loading of more than 2.5 wt% resulted in the blockage of the active centers, leading to loss of activity of catalyst [19].

Moreover, the addition of Ce promoter on Ni/SBA-16 catalyst in dry reforming reaction of methane demonstrated that there is a strong interaction between Ni and Ce and reduction with H_2 leads to improvement of the catalyst as a result of uniform distribution of the nickel particle size within mesoporous SBA-16 [29].

Ce–ZrO_2 supported metal catalysts have also been investigated previously in the CO_2-reforming of methane [33–35]. The Pt/ceria-doped zirconia catalysts showed higher activity and stability compared to Pt/Al_2O_3 catalysts [35]. The enhancement of the activity and the stability by Ce incorporation into catalyst in the CO_2 reforming reaction has been attributed to the high amount of oxygen vacancies on the support lattice near the metal particles. The cycle of reduction and dissociative oxygen chemisorption capacity of Ce–ZrO_2 was shown to be fundamental for removal of carbonaceous deposits on the active phase of surface [34].

Considering previous positive findings about Ce and Cu promoter in CO_2 reforming of methane as close reaction system to POM with synthesis gas as the same product, it is expectable to obtain similar advantageous behavior with a promoted catalytic material composed of SBA-16 supported Ni catalyst. Ce

promotion of Ni catalyst could enhance removal of carbonaceous deposits from the active center of surface [34, 35] and resulted in better dispersion of Ni due to strong interaction between Ni and Ce [29]. Promotion by Cu decreased carbon deposition in POM on SBA-15-based Ni catalyst [19]. SBA-16 as a support has demonstrated better resistance of nickel particle against sintering and improvement of activity stability [30].

The simultaneous promotion of Ni catalyst with Ce and Cu may be accompanied with a synergistic effect on the catalytic behavior.

In this study, the effect of Ce, Cu and Ce–Cu promoters on the performance of Ni/SBA-16 catalyst in the partial oxidation of methane reaction was investigated. Different prepared catalysts were examined in POM reaction to study how the above-mentioned effects influence the kinetic of POM reaction carried out onto the prepared catalysts.

Experimental

Catalysts preparation

In the first step, we synthesized the SBA-16 support following the reported method by Zhao et al. [36]. In a typical synthesis, 2.65 g of triblock copolymer F127 (Aldrich, $EO_{106}PO_{70}EO_{106}$) was dissolved in 17.4 mL of a 1.5 M HCl aqueous solution. Then, the solution was stirred at 40 °C for 2 h, and 8.75 g of tetraethyl ortho-silicate (TEOS, Merck, 99% purity) was added to the above mixture with vigorous stirring at 40 °C for 20 h. The molar composition ratios of the reagents in the mixture of synthesis were 1 TEOS:0.005 F127:5 HCl:175 H_2O. The mixture obtained was transferred into a Teflon bottle and kept at 80 °C for 48 h. The solid product was filtered, washed by deionized water and dried and was finally calcined at 550 °C for 6 h in air.

Metal loading on the silica supports modified were prepared by an impregnation method. Nickel nitrate hexa-hydrate ($Ni(NO_3)_2{\cdot}6H_2O$), $Cu(NO_3)_2{\cdot}3H_2O$ and $Ce(NO_3)_3{\cdot}6H_2O$ were used as Ni, Cu and Ce precursors.

For the preparation of Ni/SBA-16 catalyst with 9.1 wt% nickel loading, (oxygen free basis 17.6 wt%, 9.2 mol%) 1 g SBA-16 powder was impregnated by solution which consists of 0.495 g of nickel nitrate hexa-hydrate. The prepared mixture was dried and the separated solid was calcined at 550 °C for 6 h in N_2 flow.

In the same way, the promoted Ni/SBA-16 catalysts were also prepared by solutions containing the required amounts of Ce, Cu & Ce-Cu nitrate with the mole ratio $\frac{Ni}{Cu} = \frac{Ni}{Ce} = \frac{1}{1}$.

Catalyst activity test

Catalysts were evaluated in the POM reaction, which was carried out under atmospheric pressure in a fixed bed quartz reactor. In order to increase thermal resistance, catalysts were diluted by Bentonite (inert) in a catalyst/inert mass ratio of

1:1 and then they were pressed into small particles of mesh 40–60 followed by calcination at 550 °C for 6 h in N_2 flow and loaded into a quartz reactor. Before POM experiments, the catalysts were reduced in the flow of hydrogen gas at 750 °C (10 °C/min) for 3 h, and then cooled to 700 °C. After that, the reactant gas feed containing of a mixture of CH_4 and O_2 with the molar ratio of CH_4:O_2 = 2: 1 was entered into the reactor and space velocity of the total gas mixture was fixed at 18,000 mL/g_{cat} h. The activity tests were measured from 700 to 850 °C with temperature steps of 50 °C. At the outlet of the reactor, a cold vapor trap was used to condense water vapor from the product gas stream. The production of gases was analyzed by an on-line gas chromatography (Agilent 7890A), which equipped with a TCD detector and a HP-PLOT MoleSieve capillary column of 60 m in length and 0.32 mm of inner diameter with He as the carrier gas. Finally, the obtained data were used to calculate conversions (X) and molar yields (Y) based on the following equations:

$$X_{CH_4} = \frac{CH_{4(in)} - CH_{4(out)}}{CH_{4(in)}} \times 100\% \quad (1)$$

$$Y_{H_2} = \frac{H_{2(out)}}{2CH_{4(in)}} \times 100\% \quad (2)$$

$$Y_{CO} = \frac{CO_{(out)}}{CH_{4(in)}} \times 100\% \quad (3)$$

Here in and out subscripts indicate the inlet and outlet flow.

Catalyst characterization

The phase structures of the support and catalysts was determined with powder X-ray diffraction analysis (XRD, Philips PW1730). The diffraction patterns were obtained with nickel-filtered Cu K_α radiation ($\lambda = 1.5405$ Å) at 30 mA and 40 kV with scanning speed 2° in 2θ min^{-1}. The surface areas, pore volumes and pore sizes of the samples were measured by using Micromeritics (ASAP 2020, Surface Area and Porosity Analyzer) to adsorb N_2 at − 196 °C. Prior to N_2 adsorption–desorption process, the samples were degassed at 350 °C for 4 h. The specific surface areas were calculated by applying the BET method and the pore size distributions were estimated by the BJH method with the use of the desorption branch. The morphology of catalyst particle was characterized by field emission scanning electron microscopy (FESEM) with a VEGA TESCAN instrument by using an acceleration voltage of 15 kV. The energy dispersive X-ray spectroscopy (EDX) and elemental mapping were joined to SEM, operating at 20 kV.

Results and discussion

Characterization

XRD analysis

The small-angle XRD patterns of the SBA-16 support and calcined Ni/SBA-16 catalyst were shown in Fig. 1a. The SBA-16 support showed a very sharp diffraction peak at 0.9° and two small peaks at 2θ value of about 1.3 and 1.7 corresponding to (110), (200) and (211) reflections, respectively. According to the some studies, those peaks describe mesopores SBA-16 with three-dimensional cubic (1m3m) structure [37]. Also, small-angle XRD patterns of Ni/SBA-16 demonstrated that the mesoporous cage-like structure of SBA-16 was maintained during the preparation of Ni/SBA-16 catalysts. Fig. 1b showed wide-angle XRD patterns of the

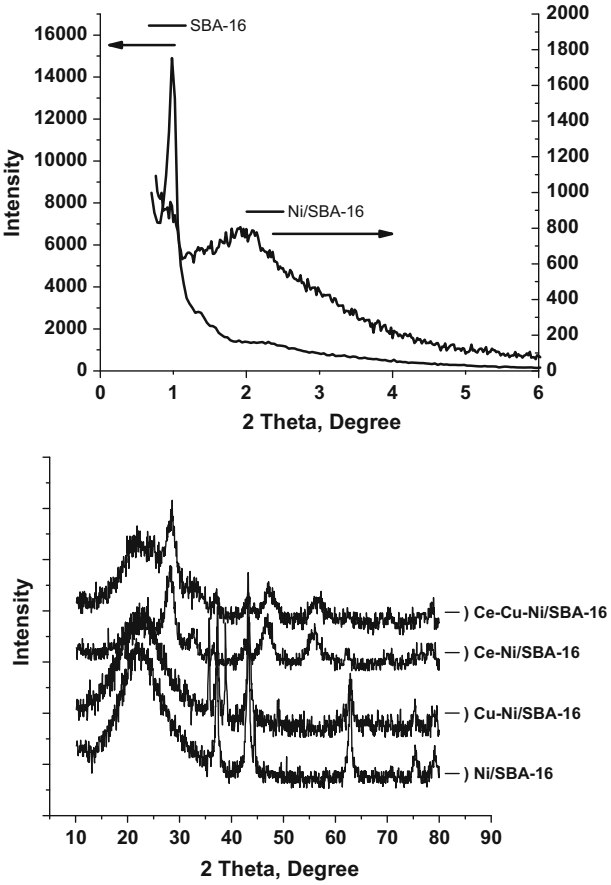

Fig. 1 Up: low-angle XRD patterns of SBA-16 support and calcined Ni/SBA-16 catalyst. Down: wide-angle XRD patterns of calcined catalysts

catalysts. As can be seen in Fig. 1b, all the catalysts showed presence of NiO peaks at 2θ values of 23.3° (broad peak), 37.2°, 43.3°, 62.9°, 75.4° and 79.6°. In comparison with other catalysts, the intensity of NiO peaks in Cu-Ni/SBA-16 catalyst showed a slight decrease. This is probably due to decrease of the dispersion of the NiO particles on the support catalysts, which was in agreement with decrease of the activity of the catalyst when was used in POM reaction. EDX data showed a slightly less Ni content (oxygen free bases) in Cu-Ni/SBA-16 compared to Ni/SBA-16, proving less exposure of Ni crystallites to reactants (less Ni dispersion) in the Cu–Ni/SBA–16.

Furthermore, the XRD patterns of Cu–Ni/SBA-16 catalyst showed two additional peaks at 2θ values around 35.6° and 38.9°, which was related to the CuO species. On the contrary, the intensity of NiO peaks showed a steep decrease For Ce–Ni/SBA-16 catalyst, suggesting that ceria could improve dispersion of the NiO particles on the support catalyst. This result was in good agreement with the activity of this catalyst. Also, Ce–Ni/SBA-16 catalyst possessed other peaks at 2θ values around 28.5°, 33.3°, 47.5° and 56.4° corresponding to monoclinic CeO species. Likewise for nickel catalyst with both promoter Ce and Cu, the intensity of NiO peaks were decreased sharply and characteristic peaks of CeO and CuO were clearly visible, although intensity of CuO peaks decreased.

Textural properties of catalysts

N_2 adsorption–desorption isotherms and pores distribution of SBA-16 support and calcined catalysts are presented on Fig. 2. As shown in Fig. 2a, these isotherms were type IV according to IUPAC classification with a hysteresis loop of type H_2 typical for materials with ink-bottle pores at P/P_o between 0.4–0.7 and 0.7–0.9, respectively; which is characteristic of the cubic cage-like pore structure [38]. As expected, after the incorporation of metal oxides on SBA-16 support, quantity of

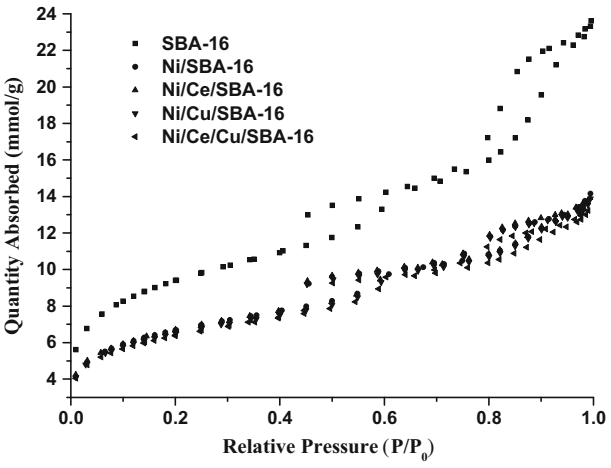

Fig. 2 N_2 adsorption–desorption isotherm of SBA-16 support and calcined catalysts

adsorbed N_2 showed an obvious decrease which revealed the decrease of pore volume of catalysts compared with pure SBA-16. Also, the existence of two hysteresis loop indicated two types of pores with different diameters. Moreover, this is seen in Fig. 2b, that the samples explained pore size distributions centered at around 3.5 and 9.5 nm. However, the small pore sizes were almost identical for pure support and catalysts, but large pore size distribution range for catalysts in comparison to pure support was narrower. On the other hand, the large pore size distribution was shifted to lower value with addition of metals to support, suggesting the incorporation of metals into large pores of support. The pore diameter, the pore volume and the BET surface area values of SBA-16 support and calcined catalysts were listed in Table 1. The specific surface area and the total pore volume of SBA-16 were 750 m^2/g and 0.79 cm^3/g, respectively. After introduction of Ni into the pores of SBA-16, the specific surface area, pore volume and pore size decreased because the NiO species were located onto the pore walls of the support porous structure. However, the properties of promoted catalysts compared to Ni/SBA-16 catalyst did not show significant change. This was due to the same content of the total moles of metals used in the preparation of catalysts.

SEM–EDX analysis

SEM images of all samples, given in Fig. 3, showed that crystallites of size 8–20 nm agglomerated to particles as large as ca. 5 μm.

EDX data of composition indicates that lower amount of metals than target value loaded onto the samples. Nickel content in all prepared samples was measured to about half of the expected amount. From the other hand, cerium content showed less difference with the target content. Copper content in the relevant samples are near to nickel content, showing the stronger adsorption of cerium compared to nickel and copper metal onto the surface of SBA-16 (Table 2).

Catalytic activity

Fig. 4 represents the catalytic performances of the prepared catalysts in the partial oxidation of methane reaction. As can be seen in Fig. 4a, For Ni/SBA-16 and Ce–

Table 1 Structural properties of SBA-16 support and calcined catalysts

Samples	Surface area[a] (m^2/g)	Pore diameter[b] (nm)	Total pore volume (cm^3/g)
SBA-16	750	3.5; 11.0	0.79
Ni/SBA-16	530	3.5; 9.4	0.46
Ce-Ni/SBA-16	526	3.5; 9.3	0.46
Cu-Ni/SBA-16	515	3.5; 9.3	0.45
Ce-Cu-Ni/SBA-16	505	3.9; 9.1	0.44

[a]Calculated by the BET equation

[b]BJH method from desorption branch

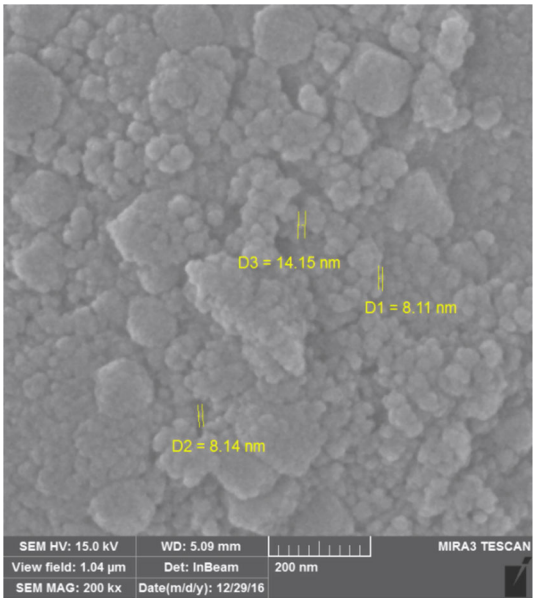

Fig. 3 SEM images of calcined catalyst Ni/SBA-16

Table 2 Composition of all calcined catalysts calculated from EDX spectra

Catalysts	Atomic % of Ni (%) (*)		Atomic % of Ce (%) (*)		Atomic % of Cu (%) (*)	
	Theoretical	Experimental	Theoretical	Experimental	Theoretical	Experimental
Ni/SBA-16	9.2	4.7	–	–	–	–
Ce-Ni/SBA-16	4.6	1.95	4.6	3	–	–
Cu-Ni/SBA-16	4.6	3.32	–	–	4.6	2.75
Ce-Cu-Ni/SBA-16	3.0	1.2	3.0	2.05	3.0	1.11

(*) Oxygen free basis

Ni/SBA-16 catalysts, CH_4 conversion showed a slight increase with reaction temperature, whereas a significant increase in CH_4 conversion was observed with Cu and with both Ce–Cu–Ni/SBA-16. This is a sign of higher activation energy of the latter catalysts.

The Ni/SBA-16 (Ni content = 5 mol%) catalyst promoted with Ce (3 mol%) showed no significant changes for the CH_4 conversion compared to Ni/SBA-16 (Ni content = 4.7 mol%) unpromoted catalyst (Fig. 6a). As indicated in Figs. 4a, 6b and c, the CH_4 conversion, H_2 and CO yields at 850 °C with Ce–Ni/SBA-16 reached to 92.5, 48 and 61.7%, respectively. Cerium may cause better dispersion of Ni on the catalyst surface, so the quantity of the active sites of catalyst remains comparable to that of Ni/SBA-16. The addition of Cu with the same molar ratio

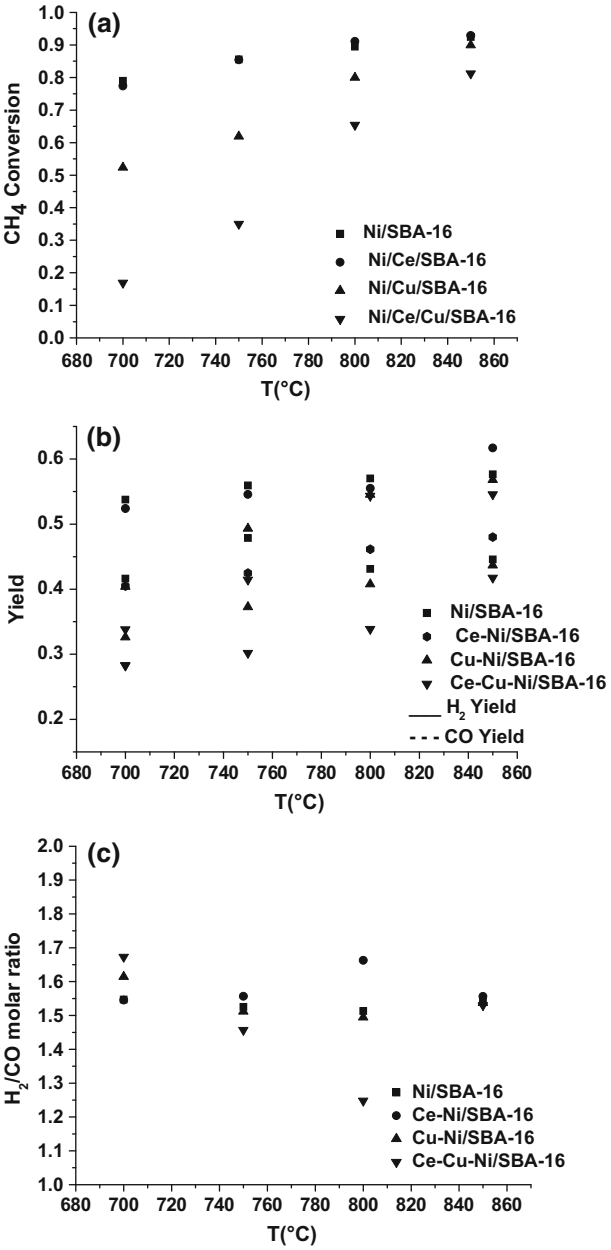

Fig. 4 **a** CH_4 conversions, **b** CO and H_2 yield **c** H_2/CO molar ratio with temperature during POM reaction over catalysts. Reaction condition: GHSV = 18,000 ml/g h, $CH_4/O_2 = 2$, catalyst loading of 200 mg

resulted in the increasing trend of CH_4 conversion with the temperature. On the contrary, in this case, the decreased amount of Ni led to the reduced conversion at the same temperature. This may be related to the decreased amount of Ni loading that accompanied by Cu loading that led to its low reactivity, although this issue is not be observed in the case of Ce–Ni/SBA-16 catalyst. It was concluded that Cu had no similar positive effect on the dispersion of Ni in the porous structure of SBA-16.

The addition of Cu and Ce together with molar ratio Ni:Cu = Ni:Ce = 1:1 led to decreased conversion of CH_4 because of much lower nickel content than other catalysts. It seems that high conversion of methane in the presence of cerium needs to a less amount of nickel. It seems reasonable with respect to the known activity of cerium oxide in providing atomic oxygen for POM reaction, but copper did not demonstrate this characteristic under the similar reaction condition. Another reason could be possibility of alloy formation of nickel and cerium as a metallic crystallite, whereas copper may segregate on the surface of nickel crystallites, preventing reactants from accessing to nickel active site. Nevertheless, reducing the amount of nickel (much lower nickel content) in the three-metallic catalyst (Ce–Cu–Ni/SBA-16 catalysts) led to a significant reduction in the conversion of CH_4 compared with the catalyst promoted by copper alone.

The following reactions proceed in the POM conversion:

$$CH_4 + 0.5\,O_2 \rightarrow CO + 2\,H_2 \quad (1)$$

$$CH_4 + O_2 \rightarrow CO_2 + 2\,H_2 \quad (2)$$

$$CH_4 + 2\,O_2 \rightarrow CO_2 + 2\,H_2O \quad (3)$$

$$CO_2 + H_2 \rightarrow CO + H_2O\ (\text{RWGS}) \quad (4)$$

The H_2/CO molar ratio on all the catalysts at the different reaction temperatures were presented in Fig. 4c. The H_2/CO molar ratio reached to about 1.55 with increasing reaction temperature on each catalyst. It may be caused by the enhancement of the reverse water gas shift (RWGS) reaction at higher temperature.

Also, the H_2/CO molar ratio did not significantly change with the reaction temperature on Ni/SBA-16 catalyst with respect to the ratio obtained at 850 °C.

The reverse slopes of H_2/CO ratio of Ce–Ni/SBA-16 and Ce–Cu–Ni/SBA-16 versus temperature at each sides of 800 °C suggested the reducing effect of RWGS reaction on H_2/CO ratio depended on the temperature with different slopes for the above mentioned catalysts. It means that the dry reforming enhances stronger than RWGS at the temperature less than 800 °C with Ni–Ce/SBA-16 catalyst whereas RWGS intensifies faster at 850 °C. The H_2/CO ratio with Ce–Ni/SBA-16 catalyst decreased after an initial increasing trend, in contrarily to the trend seen with the other catalysts. However, the reducing effect of RWGS reaction on the H_2/CO ratio became dominant at 850 °C Ce–Ni/SBA-16.

Fig. 5 shows the effect of gas hour space velocity (GHSV) on the catalytic behavior of Ni/SBA-16 catalyst at 850 °C and at the constant feed ratio of $CH_4/O_2 = 2$. As can be seen in Fig. 5, the highest CH_4 conversion amount was obtained for the lowest GHSV (9000 mL/g h), but with increasing space velocity, CH_4

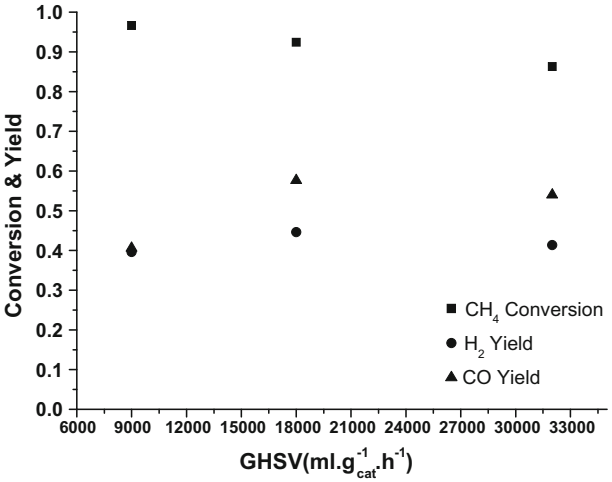

Fig. 5 Effect of GHSV on catalytic activities during POM reaction over Ni/SBA-16 catalyst. Reaction conditions: T = 850 °C, $CH_4/O_2 = 2$, catalyst loading of 200 mg

conversion was decreased because of shorter contact time between the reactant feed and the catalyst. However, the lowest H_2 and CO yields were resulted in the lowest GHSV (9000 mL/g h). Because at the lower space velocity (longer residence time), more hydrogen a in the catalyst bed reacts with the adsorbed oxygen on the surface and more coke grows through adsorbed atomic carbon. Also, Fig. 5 shows that by increase of the space velocity from 18,000 to 32,000 mL/g h, H_2 and CO yields decreased due to the reduced contact time.

The catalytic performance of Ni/SBA-16 and Ce–Ni/SBA-16 catalysts versus temperature at the different feed CH_4/O_2 molar ratios of 1.5, 2, and 2.5 is illustrated in Fig. 6. The results demonstrated CH_4 conversion over unpromoted catalyst with feed ratio of $CH_4/O_2 = 2$ was the highest, but CH_4 conversion for catalyst containing Ce at feed ratio $CH_4/O_2 = 1.5$ was the highest which was slightly larger than that of $CH_4/O_2 = 2$.

Oxygen rich feed resulted in the higher CH_4 conversion on Ce–Ni/SBA-16 with respect to Ni/SBA-16. It may be explained via stronger resistance of the latter against oxidation due to the oxygen adsorbing and releasing role of ceria.

According to Fig. 6c and d, yields of H_2 and CO on both catalysts were larger with the Oxygen rich feed. The higher is oxygen content, the higher is Yields of H_2 and CO with both catalysts.

The performance of the prepared catalysts in the POM reaction is compared to that of reported catalytic systems in Table 3. Although the experiment conditions are not identical, the synthesized catalysts with no promoter and with Ce promoter presented comparable methane conversion to the best of reported performances. However, there is a gap between CO selectivity of the prepared catalysts with the best reported values. It means that reverse water gas shift and/or total oxidation of methane is more intensified onto the prepared catalyst. The most similar catalytic material reported in Table 3, i.e. 12.5%Ni/2.5%Cu/SBA-15 shows better initial CH_4

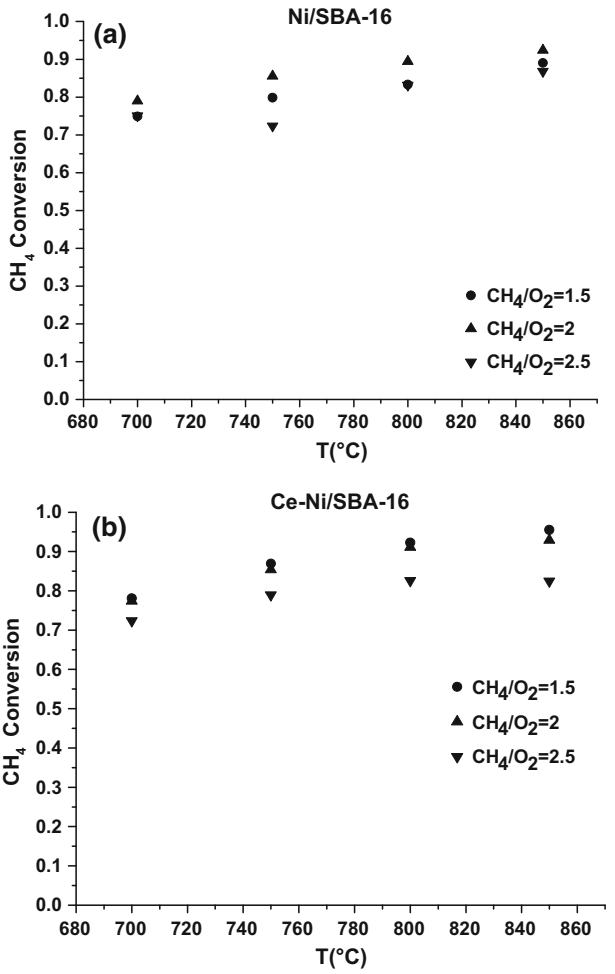

Fig. 6 CH_4 Conversion versus temperature at the different CH_4/O_2 molar ratio of feed in POM reaction over Ni/SBA-16 (**a**) and Ce-Ni/SBA-16 (**b**) catalysts. Reaction condition: GHSV = 18,000 ml/g h, catalyst loading of 200 mg

conversion and CO selectivity, but researchers did not present the duration of catalyst stability while the prepared SBA-16 supported catalyst in this work remained stable for at least 3 h. A longer independent stability test could not be carried out in this work. The stability of Ni/Ce/SBA-16 could be a result of stronger interaction of Ni crystallites with cubic mesoporous SBA-16 silica rather the hexagonal one (SBA-15). The stronger interaction with support results in smaller Ni crystallites and keeps them at the same size and activity at the severe conditions of POM reaction. Carbon formation onto all prepared catalysts was obvious regarding the black color of spent catalyst.

Table 3 Comparison of performance of reported catalytic systems with the prepared catalysts in the POM reaction

Catalyst	$X_{CH_4,i}$ [a] (%)	$X_{CH_4,5}$ [b] (%)	CO sel. (%)	H_2/CO	WHSV (ml/g h)	Temp. (°C)	CH_4/O_2	Diluent in feed (mol%)	Stability (h)	Catalyst weight (g)	References
$2Pt–CeO_2^{CD}$	96	98	99	2.0	80,000	800	2	85%	> 6	0.060	[39]
$1.8Pt–CeO_2^{HT}$	90	87	83	1.9							
$2Pt–CeO_2^{imp}$	38	23	78	1.7							
$1.9Pt–CeO_2^{CoPre}$	35	25	73	1.7							
$BaNi_yAl_{12-y}O_{19-\delta}$ (y = 0.3)	90	90	95		12,000	850	2	= 0	> 100	0.500	[13]
5%Ni–Ce(La)O_2	96		90		20,000	700	2	95.5			[15]
	89		84			650		95.5	< 100		
	84		76					94.4	= 10		
5%Ni/SBA–15	95		95	2.1	36,720	850	1.9	0	–	0.200	[19]
12.5%Ni/2.5%Cu/SBA-15	97		98	2.0							
Pt/Al_2O_3	62	62	78		523 h^{-1}	800	2	0	0	0.010	[25]
Pt/CeO_2	69	64	85								
Pt/ZrO_2	62	50	75								
Pt/Y_2O_3	65	63	80								
Ni/SBA-16	93		61	1.55	18,000	850	2	0	5	0.200	This work
Ni/Ce/SBA-16	93		68	1.55							
Ni/Cu/SBA-16	90		64	1.54							
Ni/Ce/Cu/SBA-16	80		67	1.54							
Ni/SBA-16	87		63	1.52	32,000						

[a] Initial CH_4 conversion

[b] CH_4 conversion after 5 h

Conclusions

A comparative study of performances of Ni/SBA-16 catalysts promoted by Ce, Cu and Ce–Cu were investigated for partial oxidation of methane. These catalysts with cerium, copper, copper–cerium with equimolar ratio to nickel were prepared by using an impregnation method. Characterizations of all catalysts showed that mesoporous structure of catalysts was retained after inserting metals into SBA-16 support; however, and surface area decreased. The XRD analysis revealed that dispersion of the nickel species decreased in the Cu–Ni/SBA-16 catalyst compared with other catalysts. The SEM analysis revealed similar size of nano-crystallites of catalyst samples. The activity of the Ni-SBA-16 and Ce–Ni/SBA-16 catalysts was comparable to each other with the methane conversion as high as 92.5%. The synergistic effect of cerium and nickel on the activity in POM reaction compensates for the reduced nickel content. The H_2/CO ratios of products obtained using all catalyst were higher than 1.5 at 850 °C with $CH_4/O_2 = 2$. Catalyst samples with Cu content showed inferior performance in POM reaction. Cerium promotion resulted in the higher activity with oxygen richer feed compared to the unpromoted catalyst. Catalytic activity of Ni/Ce/SBA-16 remained unchanged for 3 h at 850 °C.

The catalytic performance of synthesized catalyst in POM reaction was comparable to those reported by other researcher. Although CO selectivity was considerably lower with the prepared catalyst which could be a sign for total oxidation of methane. Carbon formation was obvious with all prepared catalysts although catalytic activity of Ni/Ce/SBA-16 was stable for 3 h and all catalyst remained stable for at least 12 h in total with 3 h stay at different temperatures.

Acknowledgements Authors gratefully acknowledge the financial support of Iran Nanotechnology Initiative Council (INIC).

References

1. Agency IETr, IEA (2010)
2. Freni S, Calogero G, Cavallaro S (2000) Hydrogen production from methane through catalytic partial oxidation reactions. J Power Sources 87(1):28–38
3. López-Fonseca R, Jiménez-González C, de Rivas B, Gutiérrez-Ortiz JI (2012) Partial oxidation of methane to syngas on bulk $NiAl_2O_4$ catalyst. Comparison with alumina supported nickel, platinum and rhodium catalysts. Appl Catal A 437:53–62
4. Elmasides C, Kondarides D, Neophytides S, Verykios X (2001) Partial oxidation of methane to synthesis gas over Ru/TiO_2 catalysts: effects of modification of the support on oxidation state and catalytic performance. J Catal 198(2):195–207
5. Melchiori T, Di Felice L, Mota N, Navarro R, Fierro J, van Sint Annaland M, Gallucci F (2014) Methane partial oxidation over a $LaCr_{0.85}Ru_{0.15}O_3$ catalyst: characterization, activity tests and kinetic modeling. Appl Catal A 486:239–249
6. Nematollahi B, Rezaei M, Khajenoori M (2011) Combined dry reforming and partial oxidation of methane to synthesis gas on noble metal catalysts. Int J Hydrogen Energy 36(4):2969–2978
7. Koh AC, Chen L, Leong WK, Johnson BF, Khimyak T, Lin J (2007) Hydrogen or synthesis gas production via the partial oxidation of methane over supported nickel–cobalt catalysts. Int J Hydrogen Energy 32(6):725–730

8. Khine MSS, Chen L, Zhang S, Lin J, Jiang SP (2013) Syngas production by catalytic partial oxidation of methane over ($La_{0.7}A_{0.3}$) BO_3 (A = Ba, Ca, Mg, Sr, and B = Cr or Fe) perovskite oxides for portable fuel cell applications. Int J Hydrogen Energy 38(30):13300–13308
9. Wang H, Ruckenstein E (2001) Partial oxidation of methane to synthesis gas over alkaline earth metal oxide supported cobalt catalysts. J Catal 199(2):309–317
10. Enger BC, Lødeng R, Holmen A (2008) A review of catalytic partial oxidation of methane to synthesis gas with emphasis on reaction mechanisms over transition metal catalysts. Appl Catal A 346(1):1–27
11. Qin D, Lapszewicz J (1994) Study of mixed steam and CO_2 reforming of CH_4 to syngas on MgO-supported metals. Catal Today 21(2–3):551–560
12. Mark MF, Maier WF (1996) CO_2-reforming of methane on supported Rh and Ir catalysts. J Catal 164(1):122–130
13. Chu W, Yang W, Lin L (2002) The partial oxidation of methane to syngas over the nickel-modified hexaaluminate catalysts $BaNi_yAl_{12-y}O_{19-\delta}$. Appl Catal A 235(1):39–45
14. Dai L-X, Teng Y-H, Tabata K, Suzuki E, Tatsumi T (2001) Catalytic application of Mo-incorporated SBA-1 mesoporous molecular sieves to partial oxidation of methane. Microporous Mesoporous Mater 44:573–580
15. Zhu T, Flytzani-Stephanopoulos M (2001) Catalytic partial oxidation of methane to synthesis gas over Ni–CeO_2. Appl Catal A 208(1):403–417
16. Claridge JB, Green ML, Tsang SC, York AP, Ashcroft AT, Battle PD (1993) A study of carbon deposition on catalysts during the partial oxidation of methane to synthesis gas. Catal Lett 22(4):299–305
17. Wang S, Lu G (1998) Reforming of methane with carbon dioxide over Ni/Al_2O_3 catalysts: effect of nickel precursor. Appl Catal A 169(2):271–280
18. Zhang Y, Xiong G, Sheng S, Yang W (2000) Deactivation studies over NiO/γ-Al_2O_3 catalysts for partial oxidation of methane to syngas. Catal Today 63(2):517–522
19. Habimana F, Li X, Ji S, Lang B, Sun D, Li C (2009) Effect of Cu promoter on Ni-based SBA-15 catalysts for partial oxidation of methane to syngas. J Nat Gas Chem 18(4):392–398
20. Kaydouh M-N, El Hassan N, Davidson A, Casale S, El Zakhem H, Massiani P (2015) Effect of the order of Ni and Ce addition in SBA-15 on the activity in dry reforming of methane. C R Chim 18(3):293–301
21. Wan H, Li X, Ji S, Huang B, Wang K, Li C (2007) Effect of Ni loading and $Ce_xZr_{ix}O_2$ promoter on Ni-based SBA-15 catalysts for steam reforming of methane. J Nat Gas Chem 16(2):139–147
22. Zhang M, Shengfu J, Linhua H, Fengxiang Y, Chengyue L, Hui L (2006) Structural characterization of highly stable Ni/SBA-15 catalyst and its catalytic performance for methane reforming with CO_2. Chin J Catal 27(9):777–781
23. Sun N, Wen X, Wang F, Peng W, Zhao N, Xiao F, Wei W, Sun Y, Kang J (2011) Catalytic performance and characterization of Ni–CaO–ZrO_2 catalysts for dry reforming of methane. Appl Surf Sci 257(21):9169–9176
24. Lucredio AF, Assaf JM, Assaf EM (2011) Methane conversion reactions on Ni catalysts promoted with Rh: influence of support. Appl Catal A 400(1):156–165
25. Passos FB, Oliveira ER, Mattos LV, Noronha FB (2006) Effect of the support on the mechanism of partial oxidation of methane on platinum catalysts. Catal Lett 110(1–2):161–167
26. Liu D, Quek XY, Cheo WNE, Lau R, Borgna A, Yang Y (2009) MCM-41 supported nickel-based bimetallic catalysts with superior stability during carbon dioxide reforming of methane: effect of strong metal–support interaction. J Catal 266(2):380–390
27. Bartholomew CH (1982) Carbon deposition in steam reforming and methanation. Catal Rev Sci Eng 24(1):67–112
28. Liu H, Li Y, Wu H, Yang W, He D (2014) Promoting effect of glucose and β-cyclodextrin on Ni dispersion of Ni/MCM-41 catalysts for carbon dioxide reforming of methane to syngas. Fuel 136:19–24
29. Zhang S, Muratsugu S, Ishiguro N, Tada M (2013) Ceria-doped Ni/SBA-16 catalysts for dry reforming of methane. ACS Catal 3(8):1855–1864
30. Park Y, Kang T, Lee J, Kim P, Kim H, Yi J (2004) Single-step preparation of Ni catalysts supported on mesoporous silicas (SBA-15 and SBA-16) and the effect of pore structure on the selective hydrodechlorination of 1,1,2-trichloroethane to VCM. Catal Today 97(2):195–203

31. Beck J, Vartuli J, Roth WJ, Leonowicz M, Kresge C, Schmitt K, Chu C, Olson DH, Sheppard E, McCullen S (1992) A new family of mesoporous molecular sieves prepared with liquid crystal templates. J Am Chem Soc 114(27):10834–10843
32. Zhao D, Huo Q, Feng J, Chmelka BF, Stucky GD (1998) Nonionic triblock and star diblock copolymer and oligomeric surfactant syntheses of highly ordered, hydrothermally stable, mesoporous silica structures. J Am Chem Soc 120(24):6024–6036
33. Stagg S, Resasco D (1998) Effect of promoters on supported Pt catalysts for CO_2 reforming of CH_4. Stud Surf Sci Catal 119:813–818
34. Stagg-Williams SM, Noronha FB, Fendley G, Resasco DE (2000) CO_2 reforming of CH_4 over Pt/ZrO_2 catalysts promoted with La and Ce oxides. J Catal 194(2):240–249
35. Noronha FB, Fendley EC, Soares RR, Alvarez WE, Resasco DE (2001) Correlation between catalytic activity and support reducibility in the CO_2 reforming of methane over Pt/$Ce_xZr_{1-x}O_2$ catalysts. Chem Eng J 82(1):21–31
36. Zhao D, Feng J, Huo Q, Melosh N, Fredrickson GH, Chmelka BF, Stucky GD (1998) Triblock copolymer syntheses of mesoporous silica with periodic 50 to 300 angstrom pores. Science 279(5350):548–552
37. Chen L, Wang S, Chen C, Zhang N (2011) Catalytic partial oxidation of methanol over Au–Pd bimetallic catalysts: a comparative study of SBA-16, SBA-16-CeO_2, and CeO_2 as supports. Transit Met Chem 36(4):387–393
38. Ma Z, Yang H, Qin Y, Hao Y, Li G (2010) Palladium nanoparticles confined in the nanocages of SBA-16: enhanced recyclability for the aerobic oxidation of alcohols in water. J Mol Catal A 331(1):78–85
39. Singha RK, Shukla A, Yadav A, Sain S, Pendem C, Konathala LSK, Bal R (2017) Synthesis effects on activity and stability of Pt-CeO_2 catalysts for partial oxidation of methane. Mol Catal 432:131–143